

**Supporting Information for:**

**High-Performance Alkaline Organic Redox Flow Batteries  
Based on 2-Hydroxy-3-Carboxy-1,4-Naphthoquinone**

Caixing Wang,<sup>†,‡</sup> Zhen Yang,<sup>‡,‡</sup> Yanrong Wang,<sup>†</sup> Peiyang Zhao,<sup>†</sup> Wen Yan,<sup>†</sup> Guoyin Zhu,<sup>†</sup>  
Lianbo Ma,<sup>†</sup> Bo Yu,<sup>†</sup> Lei Wang,<sup>†</sup> Guigen Li,<sup>‡,§,\*</sup> Jie Liu,<sup>†,||</sup> and Zhong Jin<sup>†,\*</sup>

<sup>†</sup>Key Laboratory of Mesoscopic Chemistry of MOE, School of Chemistry and Chemical Engineering, Nanjing University, Nanjing, Jiangsu 210093, China

<sup>‡</sup>Institute of Chemistry & BioMedical Sciences, Nanjing University, Nanjing, Jiangsu 210023, China

<sup>§</sup>Department of Chemistry and Biochemistry, Texas Tech University, Texas 79409-1061, United States

<sup>||</sup>Department of Chemistry, Duke University, Durham, North Carolina 27708, United States

<sup>‡</sup>These authors contributed equally.

\*Correspondence and requests for materials should be addressed to zhongjin@nju.edu.cn (Z. J.) or guigenli@nju.edu.cn (G. G. Li)

## Methods

### Chemicals

All chemicals were purchased from Sinopharm Chemical Reagent Co., Ltd with analytical grade, and were used without further purification.

### Synthesis procedures of 2,3-HCNQ

Briefly, ethyl benzoylacetate (1.72 mL, 10 mmol) and  $\text{AlCl}_3$  (4 g, 30 mmol) were dissolved in dry nitromethane (25 mL) under nitrogen. After stirring for 15 min, oxalyl chloride (0.82 mL, 10 mmol) in dry nitromethane (10 mL) was added dropwise. After 15 min, the solution was heated to 80 °C for 3 h. A solution of 10 wt.% aqueous oxalic acid (20 mL) was added under stirring at room temperature. The resulting mixture was extracted with ethyl acetate (3×15 mL). The combined extracts were treated with saturated aqueous NaCl solution (2×15 mL) and then dried with anhydrous sodium sulfate. The ethyl acetate was distilled off and the residue was chromatographed on silica gel plates (with DCM: EA from 50:1 to 20:1) to obtain the precursor 3-hydroxy-1,4-dioxo-1,4-dihydronaphthalene-2-carboxylate. A solution of the precursor in 10 wt.% aqueous KOH (50 mL) was stirred at 60 °C overnight. After cooling to room temperature, the mixture was acidified with 1 M HCl (100 mL) to form precipitation while the pH value was controlled between 2~3. The product was collected on a filter, washed with cold water for several times and dried at 70 °C overnight under vacuum. The overall yield was about 70%.

### Measurement of nuclear magnetic resonance (NMR) spectra

The  $^1\text{H}$  NMR spectra and  $^{13}\text{C}$  NMR spectra of 2,3-HCNQ were recorded on a Bruker DPX 400MHz spectrometer in DMSO with TMS as internal standard. The chemical shifts ( $\delta$ ) were reported in ppm with respect to TMS.

### Measurement of liquid chromatography-tandem mass spectrometry (LC-MS) spectra

The sample was first dissolved in  $\text{CH}_3\text{CN}$  and then filtrated by syringe filter (JinTeng 0.22  $\mu\text{m}$  Nylon 66). LC-MS analysis was performed on LCMS-2020 (Shimadzu Scientific Instrument). Electrospray ionization (ESI) mass spectra was recorded with negative ionization mode.

### **Voltammetry tests**

The CV and RDE curves were recorded using a CHI-760E workstation (ChenHua Instruments, Shanghai) by a three electrode system including a pretreated glassy carbon working electrode (polished by alumina particles with ~50 nm diameter), a platinum wire counter electrode, an Ag/AgCl reference electrode (pre-soaked in 3.0 M NaCl solution). Before the test, the solution was purged with high-purity N<sub>2</sub> for 30 minutes. For CV tests, 3 mm glassy carbon electrode (GC 130, China) was used as working electrode. RDE curves were conducted using a ALS RRDE-3A instrument equipped with a 5 mm glassy carbon working electrode. The electrode was rotated at a specific speed while the voltage linearly swept from -0.30 to -1.30 V vs. Ag/AgCl at a speed of 25 mV s<sup>-1</sup>. The diffusion coefficient (D) was determined by the slope of fitted Levich equation<sup>S1</sup>:  $i_{lim} = 0.620 nFAcD^{2/3}v^{-1/6}\omega^{1/2}$ , where  $n = 2$ , Faraday's constant  $F = 96,485 \text{ C mol}^{-1}$ , electrode area  $A = 0.196 \text{ cm}^2$ , 2,3-HCNQ concentration  $c = 2 \times 10^{-6} \text{ mol cm}^{-3}$ , kinetic viscosity  $\nu = 0.01 \text{ cm}^2 \text{ s}^{-1}$ . The rate constant ( $k_0$ ) of 2,3-HCNQ was calculated from the Tafel equation as follows:  $\log_{10}(i) = \log_{10}(nFAk_0) + \alpha nF\eta/2.303RT$ , where  $n$  is 2, universal gas constant  $R$  is 8.314 J K<sup>-1</sup>, temperature  $T$  is 293.15 K. The CV curves of 2,3-HCNQ were measured at different pH values adjusted by diluted HCl, KH<sub>2</sub>PO<sub>4</sub> and KOH solutions and calibrated by pH 4.00, 6.86 and 9.18 buffer solutions, respectively.

### **Measurement of ionization constants (pKa)**

The pKa was measured using a pH meter (pHS-3C, INESA, China) calibrated by pH 4.00 and 6.86 buffer solutions. KOH standard solution (1.026 mM) was firstly titrated by potassium acid phthalate and then added into a base burette (50.00 mL). Before the titration, 2.0 mL aqueous saturated solution of 2,3-HCNQ was diluted to 40.0 mL using deionized water (18.2MΩ, Millipore) and then purged with high-purity N<sub>2</sub> for 30 minutes, and then KOH was dropped to the 2,3-HCNQ solution with an interval of 0.10 mL. Subsequently, pH values were recorded point by point once the reading of pH meter was stable.

### **Measurement of UV-VIS absorption spectra**

All samples with different concentrations and pH values were measured using a UV-VIS spectrometer (UV-2600, Shimadzu Scientific Instrument) and quartz spectrophotometer cells

(Aldrich, 10 mm optical path length). The light wavelength was in the range of 300–800 nm with an interval of 0.5 nm.

### **Thermogravimetric Analysis (TGA)**

The TGA curve was performed on a NETZSCH STA 449C instrument under N<sub>2</sub> atmosphere from room temperature to 400 °C with a heating rate of 10 °C min<sup>-1</sup>.

### **Morphology Characterizations**

The surface structure features of pristine carbon paper (SGL 39 AA) and KOH-etched carbon paper were examined by SEM (FEI Nano Nova-450).

### **Tests of 2,3-HCNQ/K<sub>4</sub>Fe(CN)<sub>6</sub> ARFB**

The pretreated Nafion 212 membrane<sup>S2</sup> was sandwiched using three sheets of Sigracet 39 AA porous carbon paper (5cm<sup>2</sup>, which was thermally treated at 400 °C in air for 24 h and then etched by KOH/H<sub>2</sub>O (1:1 mass ratio) at 800 °C in Ar atmosphere for 1.5 h in advance, as shown in Extended Data Figure S7) at each side<sup>S3</sup>. Graphite flow fields (Shanghai Hongjun, China) connected with gold-plating copper current collectors assembled on both sides. Typically, the catholyte was prepared by dissolving potassium ferrocynaide (K<sub>4</sub>Fe(CN)<sub>6</sub>, 2.53 g, 6 mmol) into 15 mL of 1.0 M KOH solution to afford a catholyte concentration of 0.4 M. The anolyte was prepared by dissolving 2,3-HCNQ (0.55 g, 2.5 mmol) into 5.0 mL of 2.0 M KOH to afford an anolyte concentration of 0.5 M. For 1.0 M anolyte tests, 5.06 g (12 mmol) potassium ferrocynaide was dissolved into 30 mL of 1.0 M KOH as the catholyte, while 1.1 g (5 mmol) 2,3-HCNQ was dissolved into 5.0 mL of 3.0 M KOH as the anolyte. The catholyte and anolyte were purge with high-purity N<sub>2</sub> (> 99.99%) for 30 minutes and then the cell setup was put into a glovebox which was free from oxygen by continuous high purity N<sub>2</sub> flow. The electrolytes were injected into the cell at a rate of 60 mL min<sup>-1</sup> by a two-channel peristaltic pump (Zibo Newking Electromechanical Equipment, China). For cycling test (Wuhan Land Instruments, China), the battery was consecutively charged to 1.6 V and then discharged to 0.5 V at a current density of 100 mA cm<sup>-2</sup>. The SOC curve was measured by recording the open-circuit voltages after charging the battery to different states at a current density of 100 mA cm<sup>-2</sup> and then resting for 30 seconds. The ~100% SOC was obtained by charging the battery up to 1.4 V and then kept the

voltage until the current density was lower than  $5 \text{ mA cm}^{-2}$ . The polarization curve was measured at 100% SOC by linear sweep voltammetry with a scan rate of  $100 \text{ mV s}^{-1}$  using a CS1005 potentiostat electrochemical workstation with a current booster (Wuhan Corrtest Instruments, China).

#### **Tests of 2-HNQ/ $\text{K}_4\text{Fe}(\text{CN})_6$ ARFB**

The 2-HNQ/ $\text{K}_4\text{Fe}(\text{CN})_6$  ARFB was assembled following the above mentioned process, except the 2,3-HCNQ solution was replaced by 2-HNQ solution. Typically, the 2-HNQ concentration was  $0.25 \text{ M}$  ( $217.5 \text{ mg}$  of 2-HNQ dissolved into  $5.0 \text{ mL}$   $1.25 \text{ M}$  KOH solution), and the  $\text{K}_4\text{Fe}(\text{CN})_6$  solution was  $0.4 \text{ M}$ .

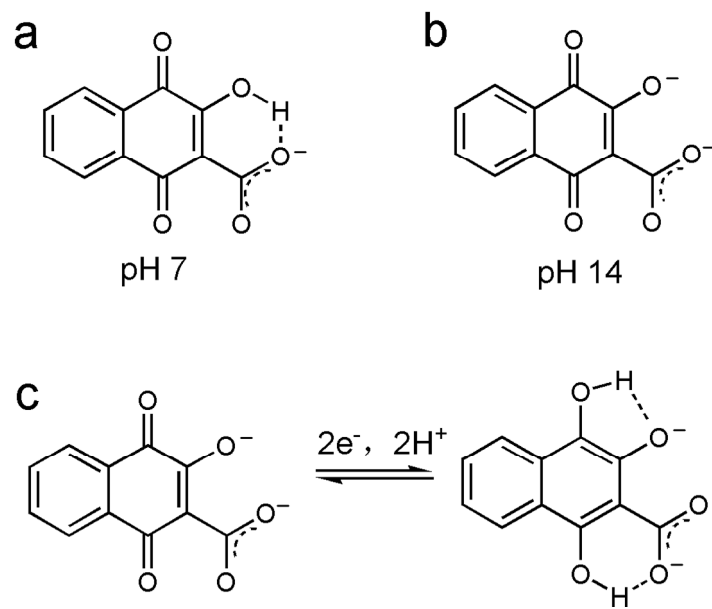
#### **Tests of 2,3-HCNQ symmetric ARFB**

Briefly,  $20 \text{ mL}$  of  $0.1 \text{ M}$  2,3-HCNQ solution was firstly charged in a 2,3-HCNQ/ $\text{K}_4\text{Fe}(\text{CN})_6$  ARFB to 100% SOC and fully discharged, and the charged to 50% SOC based on the discharge time of the 1<sup>st</sup> cycle. Subsequently, the cathode-side tank, flow channel and cell were emptied and throughoutly cleaned with pure water for several times. Then,  $14 \text{ mL}$  of anolyte solution in the anode-side tank was transferred to the cathode-side tank to perform the symmetric ARFB tests. The charge and discharge current density was set to  $30 \text{ mA cm}^{-2}$  and the cutoff voltage was  $0.3 \text{ V}$  and  $-0.3 \text{ V}$ .

**Table S1.** Performance comparisons of 2,3-HCNQ/K<sub>4</sub>Fe(CN)<sub>6</sub> ARFB in this study with other previously-reported alkaline and neutral ARFBs reported in the literatures.

Ref.	Redox materials (anolyte/catholyte)	Voltage (V)	Current density (mA cm <sup>-2</sup> )	Energy efficiency	Cycle number (n)	Capacity retention	Maximum power density (W cm <sup>-2</sup> )
This work	2,3-HCNQ/K <sub>4</sub> Fe(CN) <sub>6</sub>	1.02	100	68.6%	100	94.5%	0.255
14	2,6-DHAQ/K <sub>4</sub> Fe(CN) <sub>6</sub>	1.21	100	84%	100	90%	0.42, 0.70 <sup>a</sup>
15	Poly(MV)/Poly(TEMPO)	1.15	40	75%	100	73%	--
16	MV/4-HO-TEMPO	1.15	100	40%	100	89%	--
17	FMN/K <sub>4</sub> Fe(CN) <sub>6</sub>	1.0	50, 80	60%, 55%	200	99%	0.16
18	DHBQ/K <sub>4</sub> Fe(CN) <sub>6</sub>	1.21	100	65%	150	64%	0.32
19	ACA/K <sub>4</sub> Fe(CN) <sub>6</sub>	1.13	100	60-67%	400	90%	0.35
20	MV/TEMPTMA	1.4	50	75%	100	98.9%	--
21	MV/FcN <sub>2</sub> Br <sub>2</sub> (FcN <sub>2</sub> Cl) <sub>2</sub>	1.06	100	40%	700	91%	0.125
22	BTMAP-Vi/BTMAP-Fc	0.748	150	30%	500	99.3%	0.06
23	Zn/Poly(TEMPO)	1.7	12	40%	--	--	--
24	Zn/TEMPO-4-sulfate	1.69	40	70%	50	--	--
25	Zn/BQs	1.50, 1.58, 1.65	30	44%, 66%, 73%	12	--	--
26	[(NPr) <sub>2</sub> TTz]Cl <sub>4</sub> /N <sup>Me</sup> -TEMPO	1.44	40	70%	300	90%	--
27	1,8-DHAQ/K <sub>4</sub> Fe(CN) <sub>6</sub>	1.08	80	80%	100	80%	0.11, 0.155 <sup>a</sup>

<sup>a</sup> Temperature at 45 °C.



**Scheme S1.** (a, b) Proposed ionized structures of 2,3-HCNQ at pH 7 and 14, respectively. (c) Proposed ionized structure after the reduction of 2,3-HCNQ.

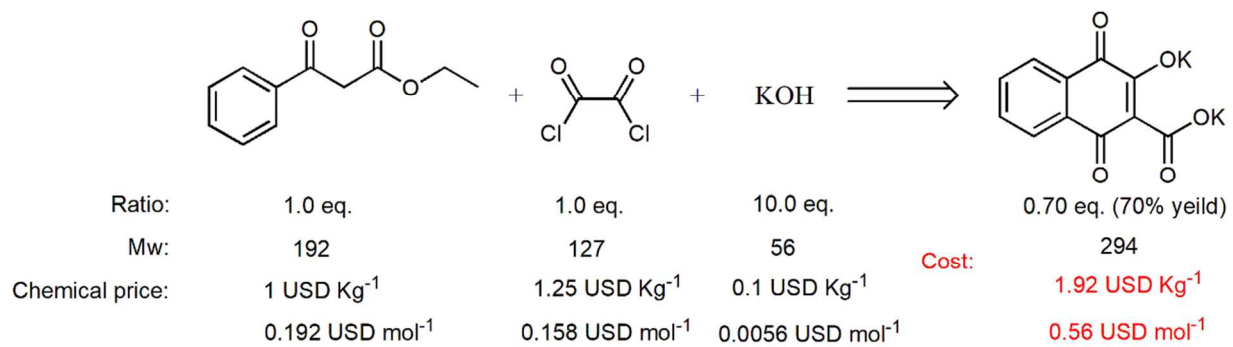


**Figure S1. Calculation of the synthesis cost of 2,3-HCNQ.** The prices of the chemicals were obtained from Alibaba.com, and the calculation method is following a previous literature<sup>S4</sup>.



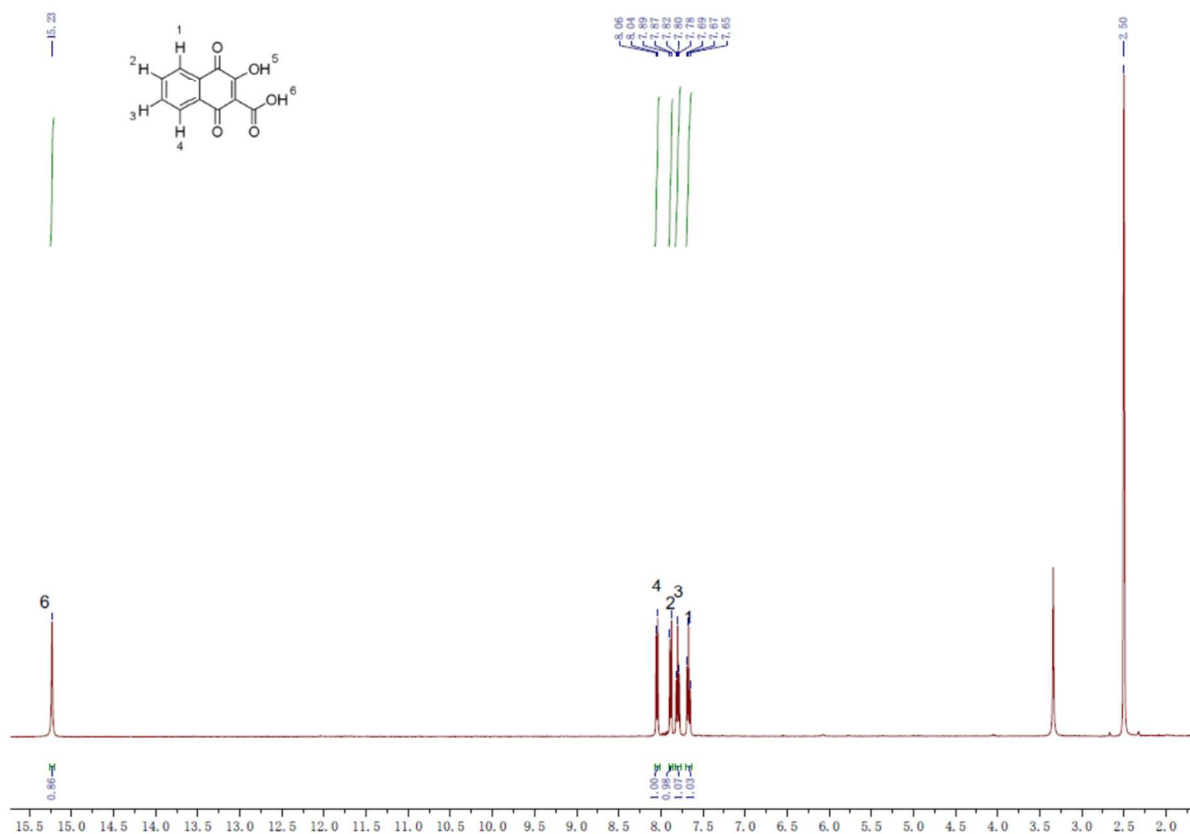


**Figure S2.** <sup>1</sup>H NMR spectrum of 2,3-HCNQ (400 MHz, DMSO).  $\delta$  15.23 (s, 1H), 8.05 (d,  $J$  = 7.7 Hz, 1H), 7.88 (d,  $J$  = 7.6 Hz, 1H), 7.80 (t,  $J$  = 7.5 Hz, 1H), 7.67 (t,  $J$  = 7.5 Hz, 1H).

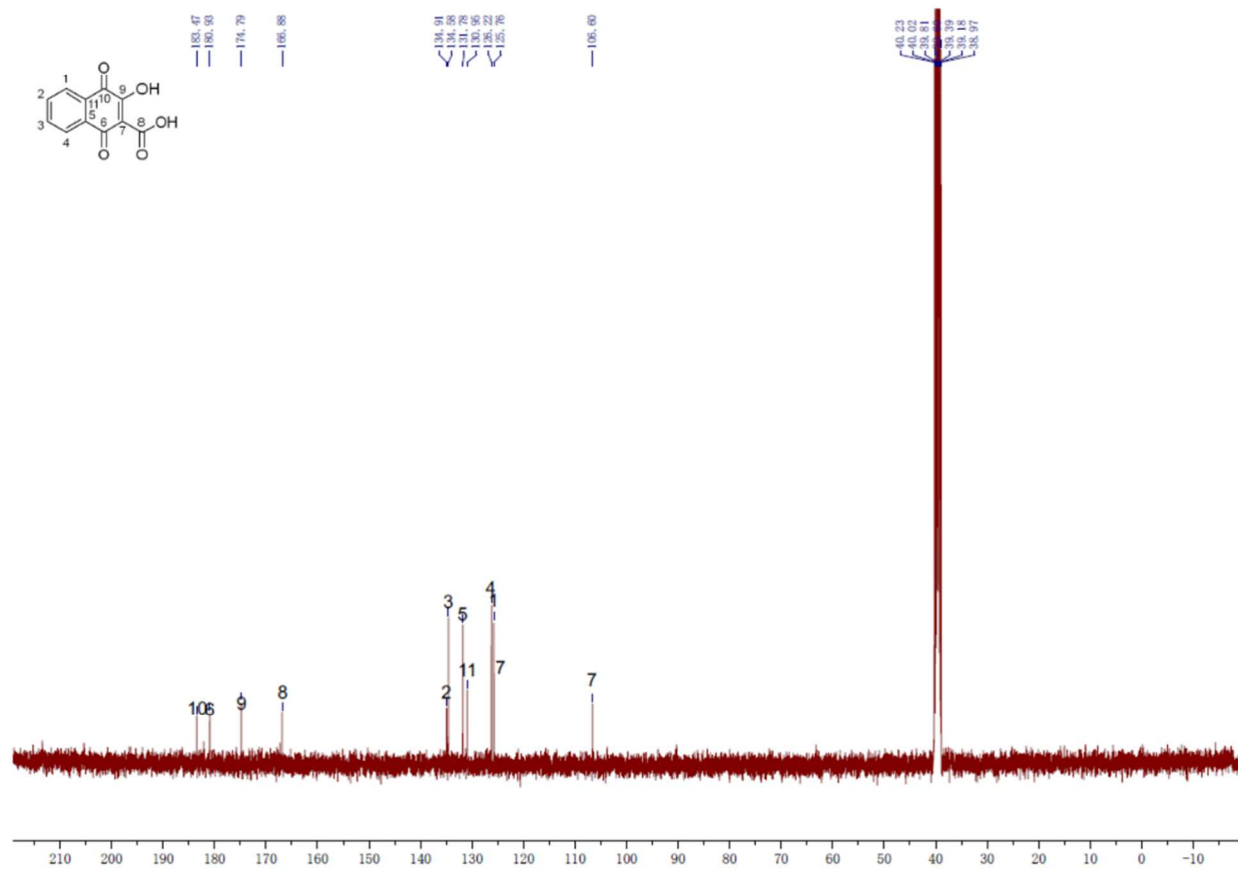


**Figure S3.**  $^{13}\text{C}$  NMR spectrum of 2,3-HCNQ.  $\delta$  183.4, 180.8, 174.7, 166.8, 134.8, 134.5, 131.7, 130.9, 126.1, 125.7, 106.5.

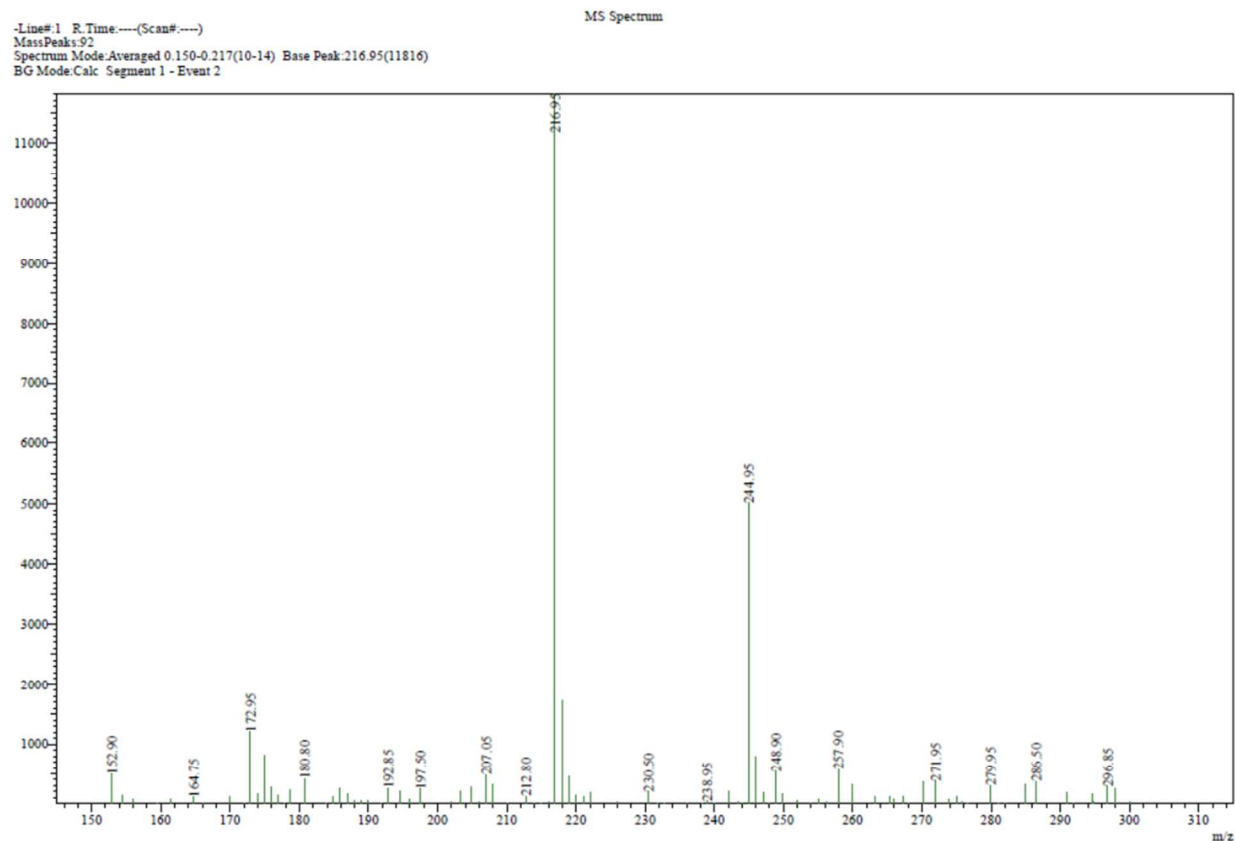
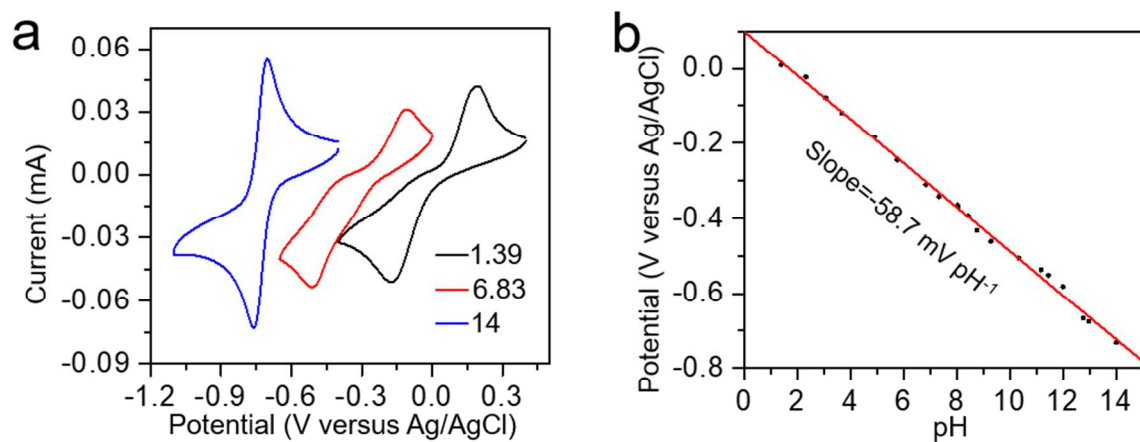
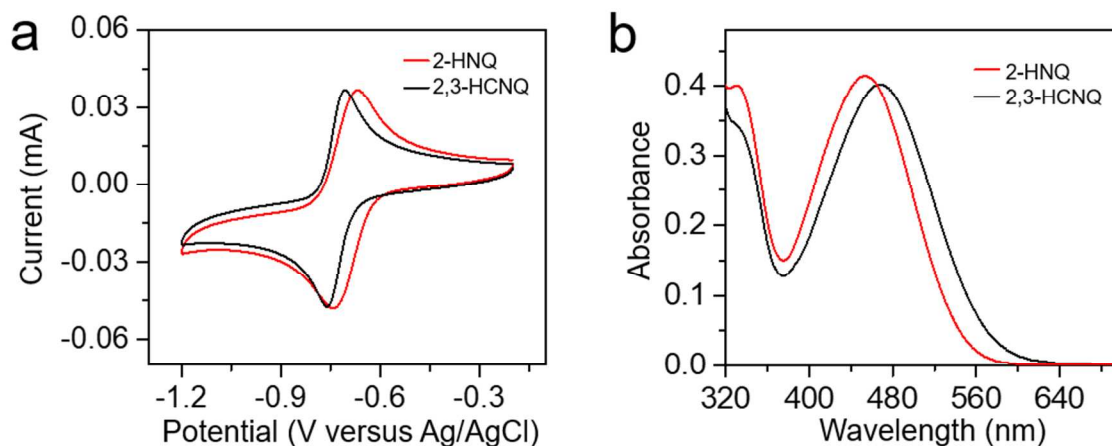


Figure S4. LC-MS spectrum of 2,3-HCNQ. M<sup>+</sup>:216.95.



**Figure S5.** (a) Representative CV curves of 2,3-HCNQ at different pH values of 1.39, 6.83 and 14, respectively. (b) Pourbaix diagram of 2,3-HCNQ in a whole range of pH values.



**Figure S6. Comparisons of the redox potentials and UV-VIS absorption spectra of 2,3-HCNQ and 2-HNQ.** (a) CV curves of 2 mM 2,3-HCNQ in 1.0 M KOH and 2 mM 2-HNQ in 1.0 M KOH. (b) UV-VIS absorption spectra of 0.2 mM 2,3-HCNQ in 1.0 M KOH and 0.2 mM 2-HNQ in 1.0 M KOH.

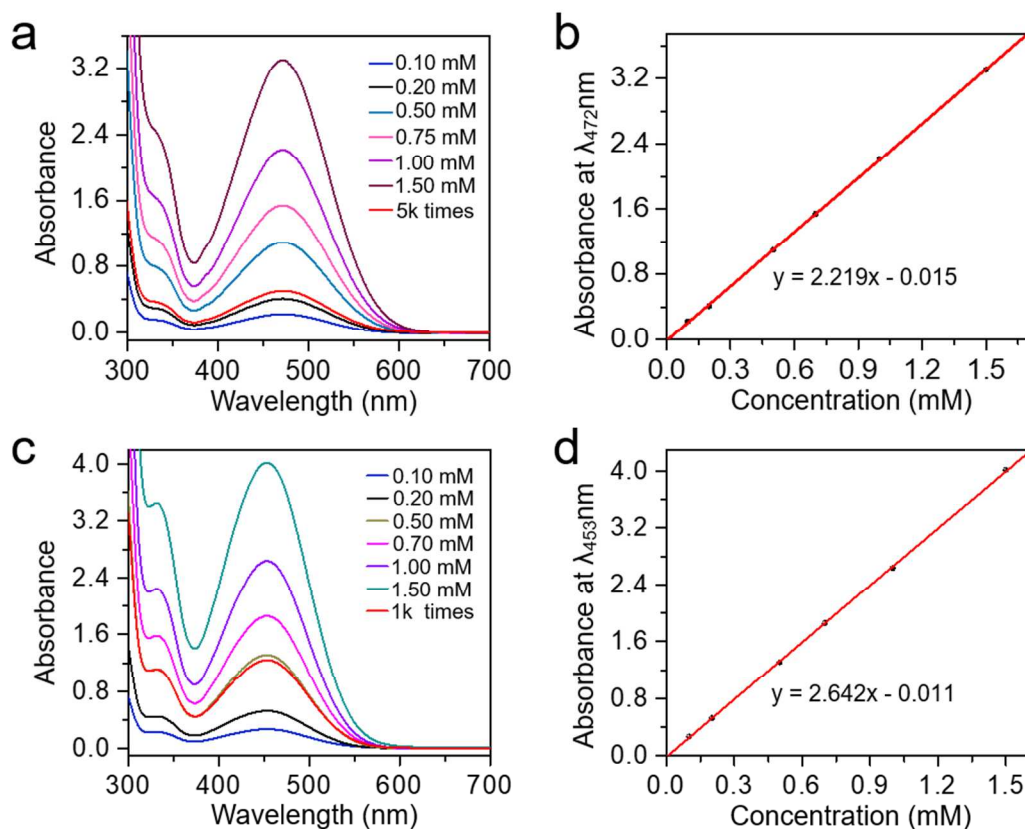


**Figure S7. Solubility measurements of 2,3-HCNQ and 2-HNQ.** (a) and (c), UV-VIS absorption spectra of 2,3-HCNQ (a) and 2-HNQ (c) solutions with different concentrations. The red traces were obtained by diluting 1.0 mL saturated solution for specific times in 1.0 M KOH. (b) and (d), the absorbance vs. concentration working curve of (b) 2,3-HCNQ at  $\lambda_{472\text{ nm}}$  and (d) 2-HNQ at  $\lambda_{453\text{ nm}}$ , respectively.

$$S_{2,3\text{-HCNQ}} = \frac{0.504 + 0.015}{2.219} \times 5000\text{ M} = 1.2\text{ M}$$

$$S_{2\text{-HNQ}} = \frac{1.241 + 0.011}{2.642} \times 1000\text{ M} = 0.47\text{ M}$$

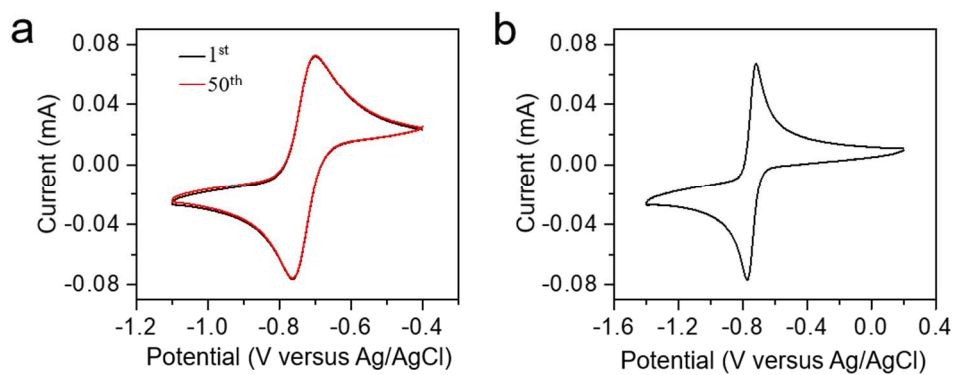


**Figure S8.** (a) CV curve of 2,3-HCNQ in 1.0 M KOH solution at a scan rate of  $100 \text{ mV s}^{-1}$  during the 1<sup>st</sup> and 50<sup>th</sup> cycles. (b) CV curve of 2,3-HCNQ in 1.0 M KOH solution within a potential range from 0.2 to -1.4 V vs. Ag/AgCl.

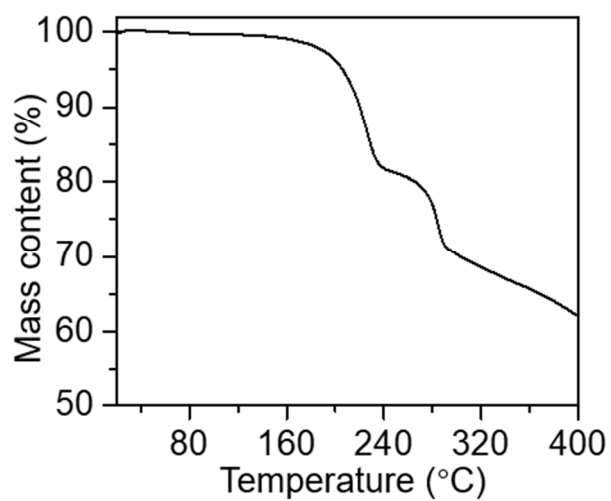


**Figure S9.** Thermal stability measurements. TGA curve of 2,3-HCNQ powder measured under N<sub>2</sub> atmosphere.



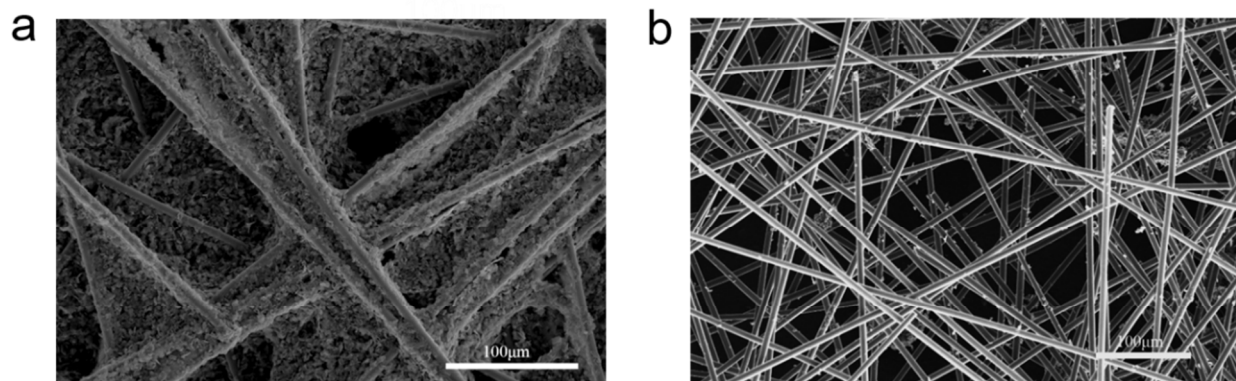


**Figure S10.** SEM images of carbon paper electrode. (a) Morphology of original carbon paper. (b) Morphology of carbon paper electrode after thermally treated at 400 °C in air for 24 h and then etched by KOH/H<sub>2</sub>O (1:1 mass ratio) at 800 °C in Ar atmosphere for 1.5 h.

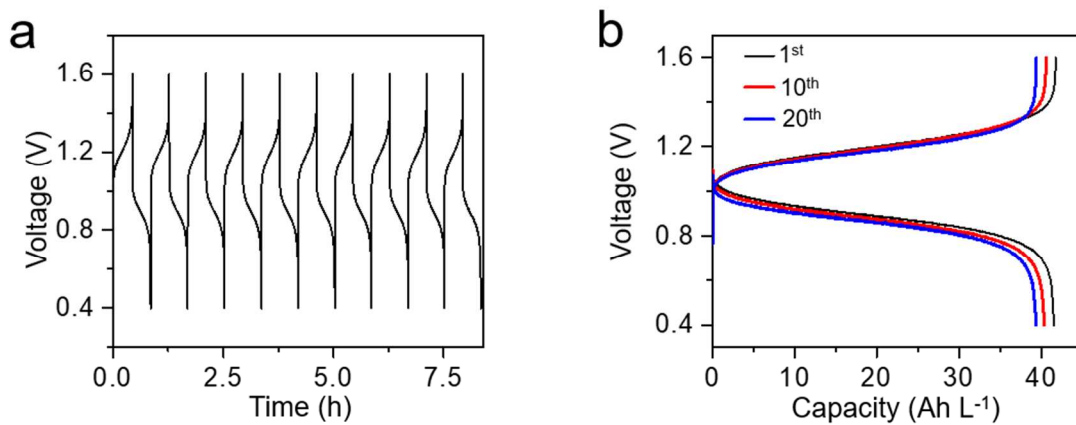


**Figure S11.** Cycle performance of 2,3-HCNQ/K<sub>4</sub>Fe(CN)<sub>6</sub> ARFB base on 1.0 M 2,3-HCNQ anolyte and 0.4 M K<sub>4</sub>Fe(CN)<sub>6</sub> catholyte. (a) Voltage vs. time curves recorded at 100 mA cm<sup>-2</sup>. (b) Galvanostatic charge-discharge curves during the 1<sup>st</sup>, 10<sup>th</sup> and 20<sup>th</sup> cycles at 100 mA cm<sup>-2</sup>.

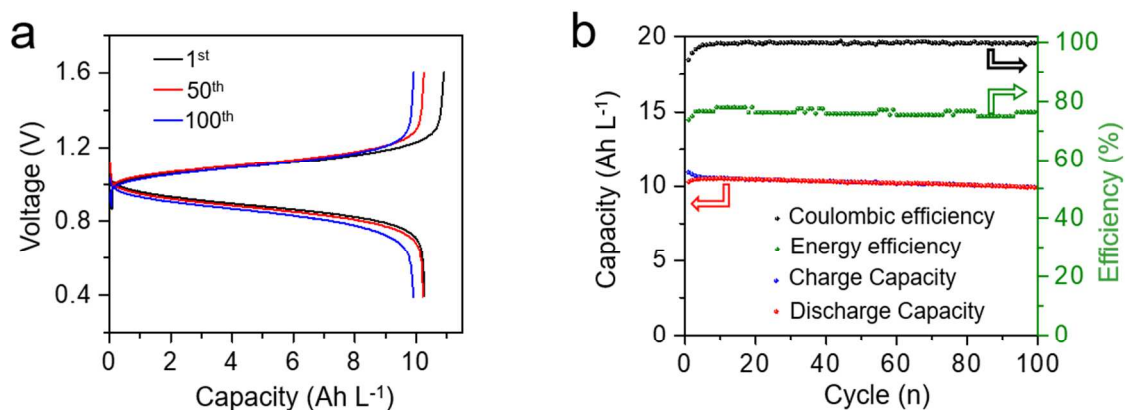


**Figure S12.** Performance tests of 2-HNQ/K<sub>4</sub>Fe(CN)<sub>6</sub> ARFB as a control experiment. (a) Galvanostatic charge-discharge curves of 2-HNQ/K<sub>4</sub>Fe(CN)<sub>6</sub> ARFB during the 1<sup>st</sup>, 50<sup>th</sup> and 100<sup>th</sup> cycles at 100 mA cm<sup>-2</sup>. The concentrations of anolyte and catholyte are 0.25 M and 0.4 M, respectively, due to the solubility limit of 2-HNQ. (b) Cycling performance, Coulombic efficiencies and energy efficiencies of 2-HNQ/K<sub>4</sub>Fe(CN)<sub>6</sub> ARFB measured at 100 mA cm<sup>-2</sup>.

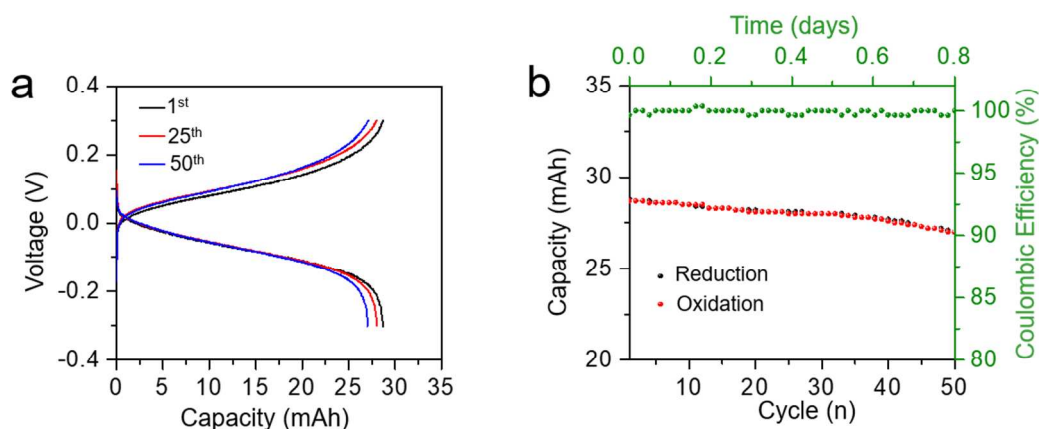


**Figure S13.** Cycle performance of a symmetric flow cell based on 0.1 M 2,3-HCNQ solution with an initial SOC of 50%. (a) Galvanostatic charge-discharge curves of 2,3-HCNQ symmetric cell during the 1<sup>st</sup>, 25<sup>th</sup> and 50<sup>th</sup> cycles at 30 mA cm<sup>-2</sup>. (b) Capacity retentions and Coulombic efficiencies of 2,3-HCNQ symmetric cell as the functions of cycle number and operation time at 30 mA cm<sup>-2</sup>.

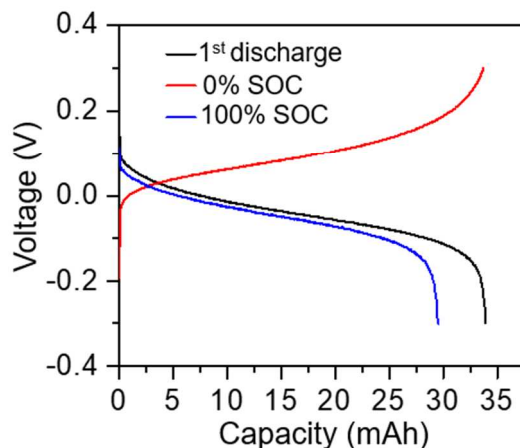


**Figure S14.** Cycling pause tests of another symmetric cell based on 0.1 M 2,3-HCNQ solution at  $30 \text{ mA cm}^{-2}$  with a resting time of 24 h at 0% SOC and 100% SOC, respectively.

## References

- (1) Treimer, S.; Tang, A.; Johnson, D. C. A Consideration of the Application of Koutecky-Levich Plots in the Diagnoses of Charge-Transfer Mechanisms at Rotated Disk Electrodes. **2002**, *14*, 165.
- (2) Orita, A.; Verde, M. G.; Sakai, M.; Meng, Y. S., A Biomimetic Redox Flow Battery Based on Flavin Mononucleotide. *Nat. Commun.* **2016**, *7*, 13230.
- (3) Zhou, X. L.; Zeng, Y. K.; Zhu, X. B.; Wei, L.; & Zhao, T. S. A High-Performance Dual-Scale Porous Electrode for Vanadium Redox Flow Batteries. *J. Power Sources* **2016**, *325*, 329.
- (4) Luo, J.; Hu, B.; Debruler, C.; Liu, T. L. A " $\pi$ -Conjugation Extended Viologen" as Novel Two-Electron Storage Anolyte for Total Organic Aqueous Redox Flow Battery. *Angew. Chem.* **2018**, *130*, 231.